Polymer Chemistry

Accepted Manuscript

ROYAL SOCIETY OF CHEMISTRY

www.rsc.org/polymers

Journal Name

RSCPublishing

ARTICLE

Synthesis and characterization of Conducting Polymers Containing Polypeptide and Ferrocene Side Chains as Ethanol Biosensors

Cite this: DOI: 10.1039/xoxxoooooox

Received ooth January 2012,
Accepted ooth January 2012

DOI: 10.1039/xoxxoooooox

www.rsc.org/

Melis Kesik[a], Huseyin Akbulut[b], Saniye Söylemez[a], Şevki Can Cevher[a], Gönül Hızalan[a], Yasemin Arslan Udum[c], Takeshi Endo[d], Shuhei Yamada[d], Ali Çırpan[a,e,f], Yusuf Yağcı[b]* and Levent Toppare[a,e,f,g]**

A novel approach for the fabrication of a biosensor with conducting polymer bearing polypeptide segments and ferrocene moieties was reported. The approach pertains to the electrochemical copolymerization of the electroactive polypeptide macromonomer and independently prepared ferrocene imidazole derivative of dithiophene (TIFc), respectively on the electrode surface. The polypeptide macromonomer was synthesized by simultaneous N-carboxyanhydride (NCA) formation and ring opening polymerization of N-Boc-L-lysine (α-amino acid of the corresponding NCA) using amino functional bis-EDOT derivative (BEDOA-6) as an initiator. Alcohol oxidase (AOx) was then covalently immobilized onto the copolymer coated electrode using glutaraldehyde as the crosslinking agent. The intermediates and final conducting copolymer before and after enzyme immobilization were fully characterized by FT-IR, 1H-NMR, GPC, cyclic voltammetry, SEM and EIS analyses. The designed biosensor combining the advantages of each component was tested as the ethanol sensing system offering fast response time (9 s), wide linear range (0.17 mM and 4.25 mM) and low detection limit (0.28 mM) with high sensitivity (12.52 μA mM $^{-1}$ cm $^{-2}$). Kinetic parameters K_M^{app} and I_{max} were determined as 2.67 mM and 2.98 μA, respectively. The capability of the biosensor in analyzing ethanol content in alcoholic beverages was also demonstrated.

Introduction

Conducting polymers (CPs) are known as "synthetic metals", making them fundamental materials in many research fields owing to their overwhelming characteristics.[1] They exhibit both excellent conductivity and high mechanical strengths and processability. The use of conducting polymers as excellent immobilization platform for biomolecules led to the development of efficient biosensors, taking the advantages of ease of processability, ability of conduct the electricity in the any desired level, low cost, straightforward preparation techniques.[2] CPs provide high surface area, adjustable morphology by arranging thickness of the polymer film and offer extensive stability of the enzymes incorporated.[3-5] Moreover, these materials also facilitate structural and electronic modifications to be used in detecting a target compound in any test solution. The polymer structure can be tuned to accomplish desired properties, producing sensitive and reproducible microenvironment for biological reactions to mimic the naturally occurring environments of biological molecules.[6] With the help of created functional groups, well organized matrices with anticipated biosensor properties can be achieved.

The elaboration of polypeptides into the polymeric structures opens new perspectives in the field of biotechnology as they are fascinating biomaterials mimicking natural proteins.[7,8] Polypeptides, possessing wonderful biocompatibility as well as remarkable mechanical and biological durability, are used to advance an excellent platform in biosensor fabrication.[9-11] Furthermore, polypeptides are assumed to exhibit a three dimensional conformation under certain conditions.[12-14] Therefore, combining synthetic polymers with polypeptide segments becomes a promising approach in the field of enzyme immobilization. The resulting feature reveals compelling self-assembling behavior[15] and new versatile functions are created through synergic effect of polymeric structures with polypeptide units. Hence, a novel design and syntheses of polypeptide containing conjugated polymers have attracted great interest. In terms of economical and practical prospects, the ring-opening polymerization of the corresponding α-amino acids of N-carboxyanhydrides (NCAs) appears to be the best technique for the synthesis of considerable variety of polypeptides by using many different nucleophiles and bases.[16-22] Although polymer chains grow linearly with monomer conversion without side reactions, the amine based initiating systems suffer from the requirement of extreme impurity-free

conditions to achieve the decisive control of a certain molecular weight and terminal structure with living nature. It was recently shown that the precursor NCAs can be obtained via intramolecular cyclization of activated urethane derivatives of α-amino acids by a simple procedure providing a practical and green way for polypeptide synthesis without the use and production of any toxic compounds. Quite recently, the method was further improved by taking advantage of consecutive NCA formation and polymerization processes by precursor urethane derivatives. Upon thermolysis in the presence of primary amines, in situ NCA formation and polycondensation with the elimination of phenol and CO_2 essentially yields desired polypeptides.[23-32]

Ferrocene derivatives are known to be excellent electron transfer mediators due to their several superior characteristics such as relatively low molecular mass, reversibility and generation of stable redox forms.[33] Development of redox polymer modified electrode has led to a worldwide interest in biosensor construction since polymers enable incorporation of reagents to the polymer backbone. Typical examples involving direct coordination of ferrocene to polymer with covalent linkage demonstrate possibility of fabrication of reagentless devices preventing leaching of the mediator.[34-36] The existing methodologies comprising non-covalent attachment of ferrocene to biosensor create problems associated with signal loss and decrease in the biosensor lifetime and analytical performance arising from the diffusion of ferrocene away from the surface into the bulk solution during enzymatic reaction.[33] Hence, considerable efforts have been directed towards development of effective biosensors by incorporating ferrocene units within the polymeric chain.

Rapid detection and quantification of alcohols with high sensitivity and selectivity play an important role in food technology. Many analytical methods based on chromatographic or spectroscopic strategies have been proposed for ethanol determination. Although these methods are routinely used in industry, they are time consuming and relatively expensive, require separation processes, and need well trained operators. Therefore, alternative approaches are being developed to overcome such problems. For this purpose, a variety of enzyme based amperometric biosensors have been proposed. Alcohol oxidase (AOx) is one of the most widely used enzyme as bio-recognition element. It is an oligomeric enzyme consisting of eight identical sub-units arranged in a quasi-cubic arrangement and each containing a strongly bound cofactor, flavin adenine dinucleotide (FAD) molecule.[37] Thus, AOx is a promising catalyst in alcohol biosensor fabrication due to its substrate selectivity and stability. Herein, we describe an electrochemically simple synthetic approach, capable of yielding random conducting copolymer possessing both polypeptide side chains and ferrocene units. To access the conjugated biopolymer architecture, first electroactive polypeptide macromonomer was prepared through simultaneous NCA formation and ring opening polymerization of N-Boc-L-lysine (α-amino acid of the corresponding NCA) using amino functional bis-EDOT derivative (BEDOA-6) as the initiator, then copolymerized with another electroactive monomer; ferrocene imidazole derivative of dithiophene (TIFc). Such combination allows well interaction between the biomolecule and conducting layer thereby improving the stability. It was then predicted that the polymer coated on the electrode provides an excellent matrix for the immobilization of AOx through the terminal amino groups of the polypeptide side chains. In a subsequent step, the matrix was fixed by using glutaraldehyde as the crosslinking agent. In this study, we demonstrate that conjugated conducting coatings based on peptide sequences in combination with ferrocene units and specific enzymes such as AOx provide a simple route to surfaces that can act as amperometric ethanol biosensor. This versatile novel coating platform is expected to be translated into a number of biosensor applications by using suitably selected enzymes.

Results and Discussion

In general, using modified thiophene compounds as monomers in electrochemical copolymerization was already applied to produce conjugated polymers composed of polythiophene main chains or side chains. In the related works from the authors' laboratories, polythiophenes or polypyrroles with various polymeric side chains, namely poly(methyl methacrylate), polytetrahydrofuran, poly(ethylene oxide), poly(ε-caprolactone) and silsesquioxane nanocages were successfully prepared to introduce additional properties such as flexibility, biocompatibility etc.[38-42] The general approach in these studies pertains to the preparation of well-defined thiophene functional macromonomers by using controlled/living radical and ionic polymerization processes and their subsequent electro copolymerization with low molar mass electroactive monomers such as thiophene and pyrrole. Quite recently, the concept was further extended to bio systems by preparing thiophene functional macromonomer possessing polyalanine.[43]

In accordance with the macromonomer concept, we carefully chose to synthesize highly conjugated bisEDOT derivative with suitable initiator functionality to form polypeptide. Thus, 6-(4,7-bis(2,3-dihydrothieno[3,4-b][1,4]dioxin-5-yl)-2H-benzo[d][1,2,3]triazol-2-yl)hexan-1-amine) (BEDOA-6) was synthesized in high yields and purity (Scheme S1). We also synthesized the monomer of urethane derivative of N-Boc-L-lysine in a single step from commercially available N-Boc-L-lysine amino acid (Scheme S2). N-Boc-L-lysine amino acid was deliberately selected so as to provide solubility in organic solvents and advantages to easily eliminate Boc group in the mild conditions for further application through the amino group if needed. Polymerization of urethane derivative of N-Boc-L-lysine by using BEDOA-6 was performed in DMAc in one pot through successive NCA formation and ring opening reactions to yield, BEDOA-6-poly(L-Boc) macromonomer (Scheme 1) with a molecular weight of M_n = 17.000 g mol-1 and polydispersity, M_w/M_n is 1.60 as determined by GPC.

The structure of the electroactive macromonomer was confirmed by 1H-NMR analysis. The spectrum presented in Figure 1 shows broad peaks at 1.79-1.33 ppm and 2.07-1.80 ppm in respect to both alkyl groups of the repeating unit and initiator. The other characteristic peaks of BEDOA-6 moiety resonate at 4.30 and 4.38 ppm.

Journal Name RSCPublishing

ARTICLE

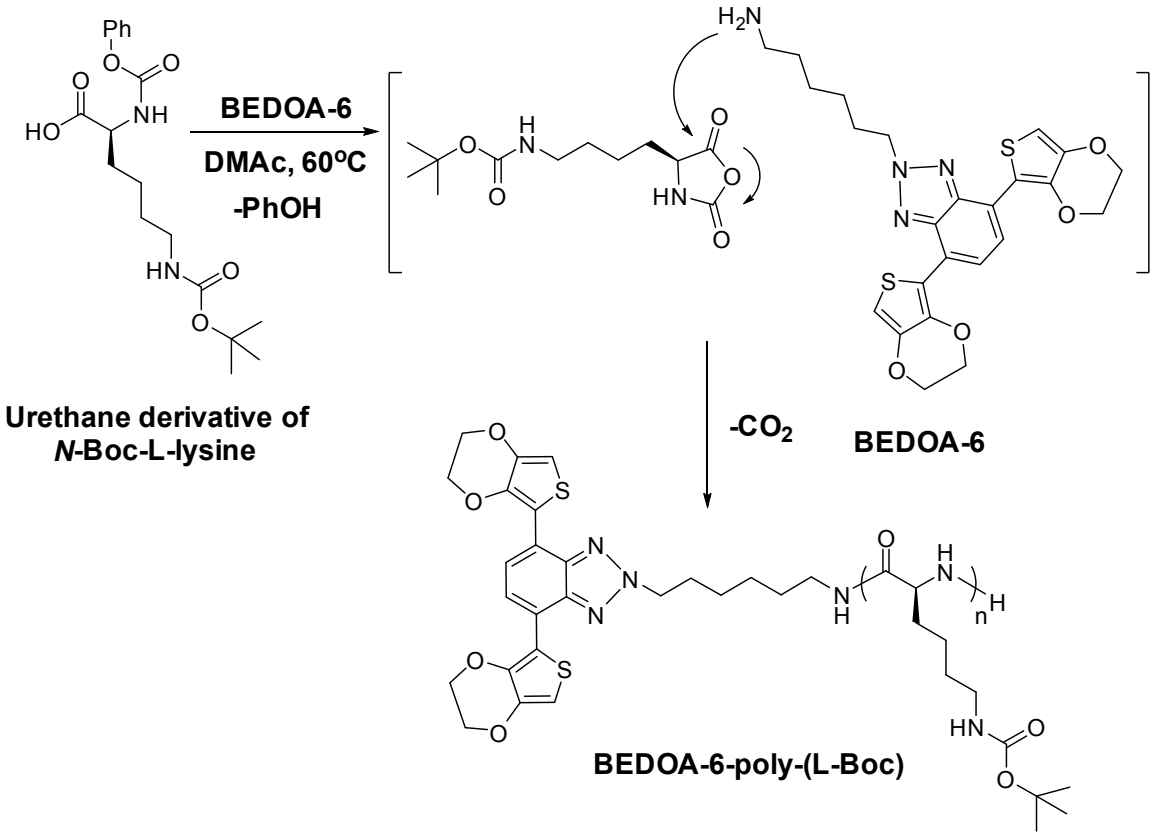

Scheme 1. Synthesis of electroactive polypeptide macromonomer, BEDOA-6-poly(L-Boc).

Electro (co)polymerization and electrochemical studies.

Electrochemical copolymerization is an efficient approach to obtain polymers having combined properties of the homopolymers. These copolymers are expected to embody the superiority of both of the parent polymers, display better coating and electrochemical properties. In order to combine polypeptide and ferrocene properties on a conducting polymer, electro copolymerization of BEDOA-6-poly(L-Boc) macronomer and TIFc was accomplished by cyclic voltammetry technique. For comparison, homo polymerization of TIFc in the absence of the macromonomer under identical experimental conditions was also performed (Scheme 2).

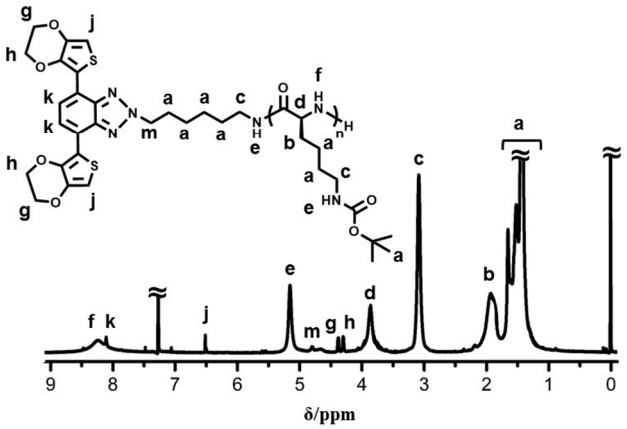

Figure 1. The 1H-NMR spectrum of BEDOA-6-poly(L-Boc)

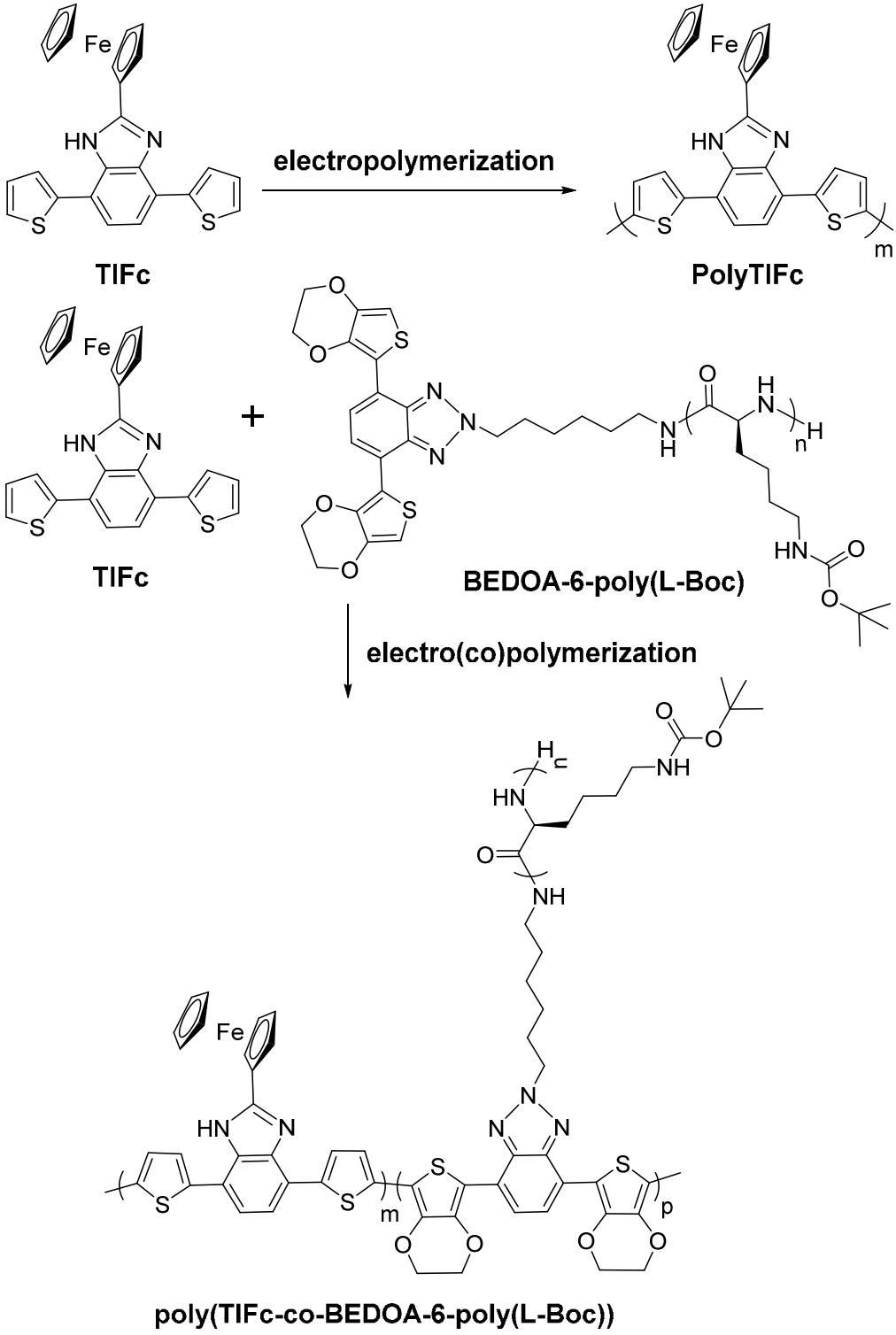

Scheme 2. Synthesis of poly(TIFc) and poly(BEDOA-6-poly(L-Boc)) by electropolymerization.

The electrochemical behavior of deposited films of the copolymer and homopolymer was studied by potential cycling between -0.20 V and +0.80 V vs. Ag wire in 0.1 M ACN/DCM (95:5) solution of $LiClO_4/NaClO_4$ (blank solution). Figure 2 displays the cyclic voltammogram of the poly(TIFc-co-BEDOA-6-poly(L-Boc)) copolymer and homo PolyTIFc films in blank solution at a scan rate of 100 mV/s respectively. The differences in blank solution responses can clearly be observed. While the homopolymer film shows two oxidation and two reduction peaks at 0.50 V/0.65 V and 0.55 V/0.34 V, respectively, the copolymer film presents the corresponding redox couples at different potentials at approximately 0.44 V/ 0.62 V and 0.54 V/ 0.40 V.

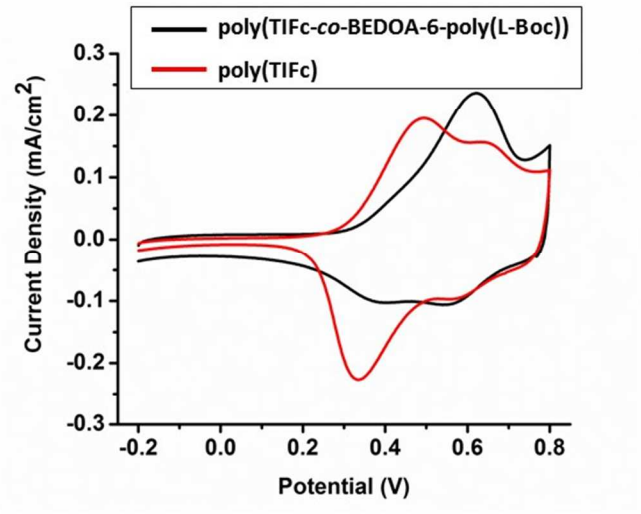

Figure 2. Single scan cyclic voltammograms of poly(TIFc) and poly(TIFc-co-BEDOA-6-poly(L-Boc)) in a monomer free 0.1 M ACN/DCM (95:5) solution of LiClO4/NaClO4.

To further confirm the electroactivity of the films thus formed on the electrode, the peak current of the copolymer was monitored in the monomer-free supporting electrolyte system as a function of scan rate during cyclic voltammetry (Figure 3A). The related anodic peak current density at 0.3 V responses are illustrated in Figure 3B. As can be seen, anodic current densities of the copolymer show a linear dependence with the scan rate. Such observation indicates that migration of the electroactive species is not diffusion controlled and the polymer film is well adhered.

FTIR-ATR

The structures of the polymers were confirmed by the ATR-FTIR analysis. Figure S1 shows the ATR-FTIR spectra of homo poly(TIFc) and poly(TIFc-co-BEDOA-6-poly(L-Boc)). In the spectrum of poly(TIFc), the characteristics ferrocene peaks appear at around 799 cm^{-1}, 1108 cm^{-1}, 1413 cm^{-1}, 3100 cm^{-1}.[44] In the copolymer spectrum, in addition to these ferrocene peaks, new bands corresponding to the polypeptide units are detected. The peak at 1168 cm^{-1} is due to C-O stretching vibration. The amide II and C=O amide stretching bands resonate at 1545 cm^{-1} and 1698 cm^{-1}, respectively.[45] The peaks at 2934 cm^{-1} and 3293 cm^{-1} are assigned to free amino acid C-H stretching and –NH2 stretching vibration, respectively. The presence of conjugated backbone stemming from both monomer and macromonomer sequences was also confirmed. The signals at 1267 cm^{-1}, 1412 cm^{-1} and 1435 cm^{-1} are associated with N=N stretching, C-N stretching and C-H deformation vibration, respectively. Aromatic conjugated C=C stretching vibration is observed at 1651 cm^{-1}.[46] The peak at 2978 cm^{-1} corresponds to C-H stretching vibration. These observations verify that both monomer and macromonomer take part in the electrochemical process and the resulting copolymer possesses their prominent features.

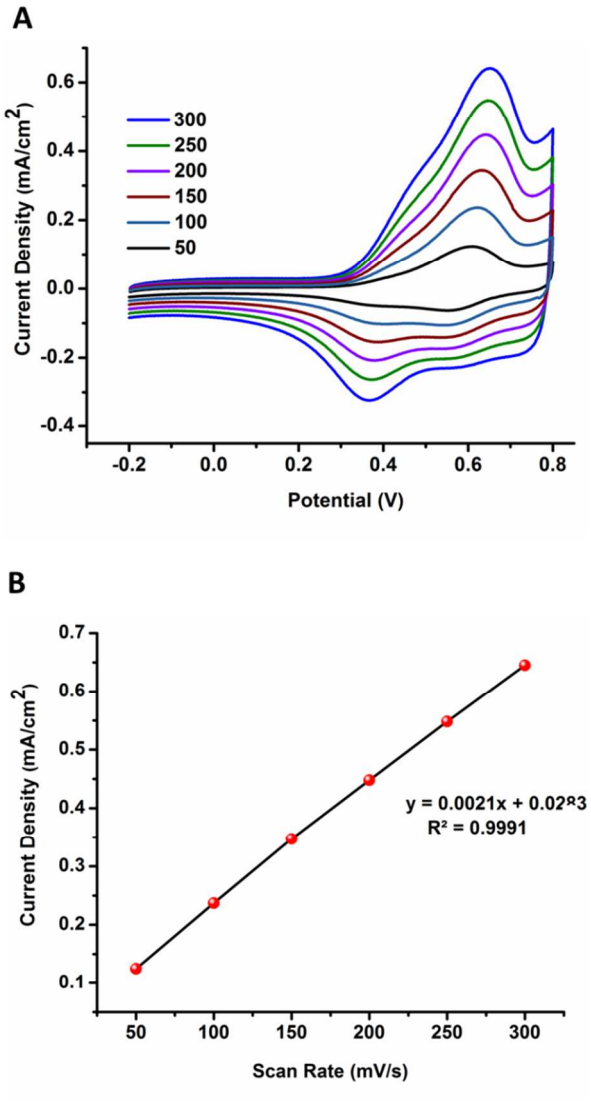

Figure 3. Cyclic voltammograms of (A) poly(TIFc-co-BEDOA-6-poly(L-Boc)) film in 0.1 M NaClO4/LiClO4/DCM/ACN (5/95, v/v) at scan rates of 50, 100, 150, 200, 250 and 300 mV/s. (B) Correlation between scan rate and peak current of the film.

Journal Name RSCPublishing

ARTICLE

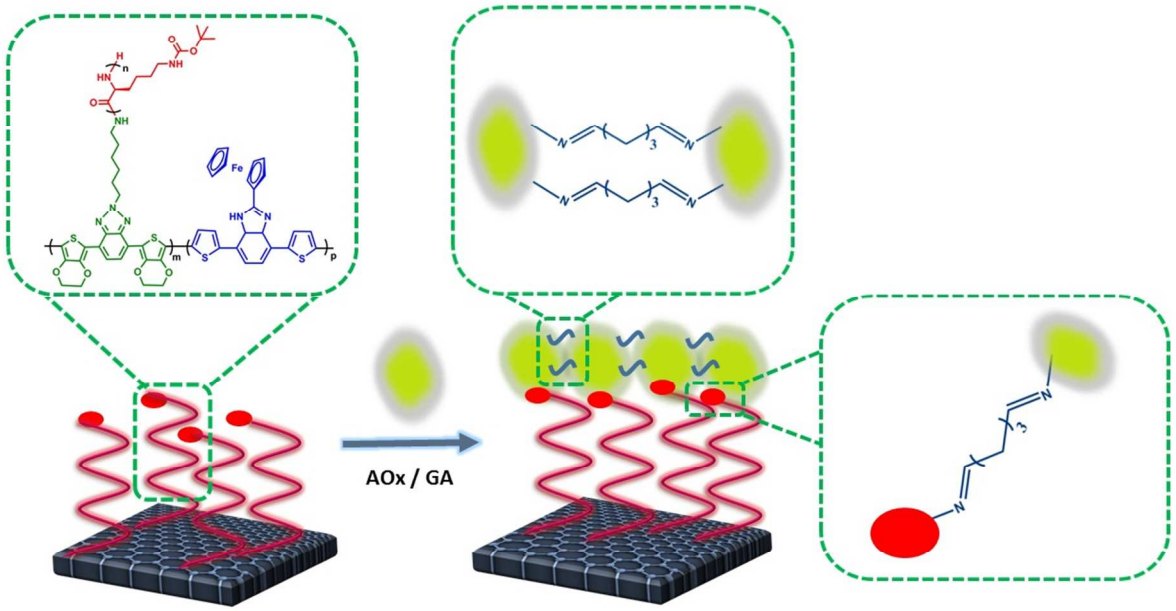

Scheme 3. Preparation of the amperometric ethanol biosensor for poly(TIFc-co-BEDOA-6-poly(L-Boc)).

Optimization of experimental parameters

Effect of poly(TIFc) and poly(TIFc-co-BEDOA-6-poly(L-Boc)) films on biosensor performance was investigated. For this purpose, two different biosensors were prepared using different polymer films while all parameters were kept constant. Scheme 3 depicts the construction procedure of the amperometric ethanol biosensor for poly(TIFc-co-BEDOA-6-poly(L-Boc)).

As shown in Figure 4A, the enzyme electrode prepared with copolymer film exhibited the highest biosensor performance. It can be easily seen that presence of only ferrocene moieties on the electrode surface do not reveal the biosensor performance as good as the one in the presence of copolymer films. Although ferrocene containing conducting polymer film facilitate the biosensor performance with mediator characteristic, it is not enough to bring about an appropriate platform for enzyme deposition. On the other hand, it was observed that when a biosensor with the incorporation of the polymeric structures bearing polypeptide segments was fabricated, biocompatible chains led to increase biosensor performance, providing three-dimensional microenvironment for biomolecules. Moreover, poly(TIFc-co-BEDOA-6-Poly(L-Boc)) copolymer film enables the formation of covalent bond during immobilization step owing to its bearing pendant amino groups which create a robust and efficient conjugation between enzyme molecules. Thus, this strong attachment enhanced retention of biocatalytic activity. Accordingly, performance of the biosensor was improved by the addition of mediators in immobilization matrix. Also, good film forming capability of poly(TIFc) make the immobilization platform excellent for biomolecules deposition by providing appropriate morphology. Hence, the interests of each polymeric structure were combined via copolymerization and used in the same platform, achieving an excellent alcohol biosensor.

Thickness of the copolymer film was adjusted by the duration of electro copolymerization in terms of charge passing through the cell.[47] To detect optimum thickness of the copolymer film, the bare graphite electrodes were coated with different scan numbers. For this purpose, different biosensors with 5, 15, 25, 35 scans were prepared and their biosensor response to the substrate were compared by keeping the other parameters

constant. Since the thickness of the copolymer film is crucial, it is important to choose the most satisfying immobilization matrix for stabilization of 3D structure of enzyme molecules. If the layer in not arranged properly, diffusion problems between polymer coated electrode and biomolecule or denaturation of biomolecules may arise. As seen in Figure 4B, the highest response was recorded with 15 cycle film deposition for biosensor application which corresponds to 27.8 nm (equivalent of 0.12 mC charge) in thickness.

Activity of biomolecules is affected seriously by the pH of the working medium, optimization of pH of the buffer solution is really important. Therefore, amperometric signals were compared in the range of pH 6.0-8.5 (50 mM sodium phosphate buffer, 25ºC), using the proposed biosensor while the other preparation of biosensor parameters were kept constant. Figure 4C shows that the maximum signal was detected at pH 7.0. Hence, pH 7.0 sodium phosphate buffer was used for further experiments to improve activity of enzyme.

The effect of different amounts of AOx on biosensor performance was examined. The amounts of other components were kept constant. As seen in Figure 4D, the highest signal corresponds to 7.56 U AOx. Excess loading of enzyme resulted in leaching from the surface since enzyme molecules were not sufficiently stable onto the surface area. On the other hand, inadequate enzyme loading caused low sensitivity of the biosensor due to the low yield of enzymatic reaction. Therefore, sufficient enzyme amount should be 7.56 U to achieve stable and reasonable biosensor responses.

Biosensor characterization

Electrochemical Impedance Spectroscopy

Electrochemical Impedance Spectroscopy (EIS) was carried out to characterize the interface properties of the modified electrodes at the surface during the fabrication process of the biosensors.[48,49] Electron transfer between the solution species and the electrode surface occurs by tunneling through the barrier. In a Nyquist plot, the semicircle portion corresponds to the electron-transfer resistance at the higher frequency range which controls the electron transfer kinetics of the redox probe at the electrode surface. The semicircle diameter equals the electron transfer resistance. Such resistance controls the electron-transfer kinetics of the redox probe at the electrode interface. Moreover, linear part of the plot at lower frequency range represents the diffusion limited process. EIS study was performed on the modified electrodes in 5.0 mM $Fe(CN)_6^{3-/4-}$-containing 0.1 M KCl solution with a frequency range between1 Hz and 200 kHz via applying a constant potential of 5 mV. Figure S2 illustrates typical Nyquist plots obtained from bare electrode, poly(TIFc-co-BEDOA-6-poly(L-Boc)), poly(TIFc-co-BEDOA-6-poly(L-Boc))/AOx using $Fe(CN)_6^{3-/4-}$ as the redox probe. It can be seen that the bare

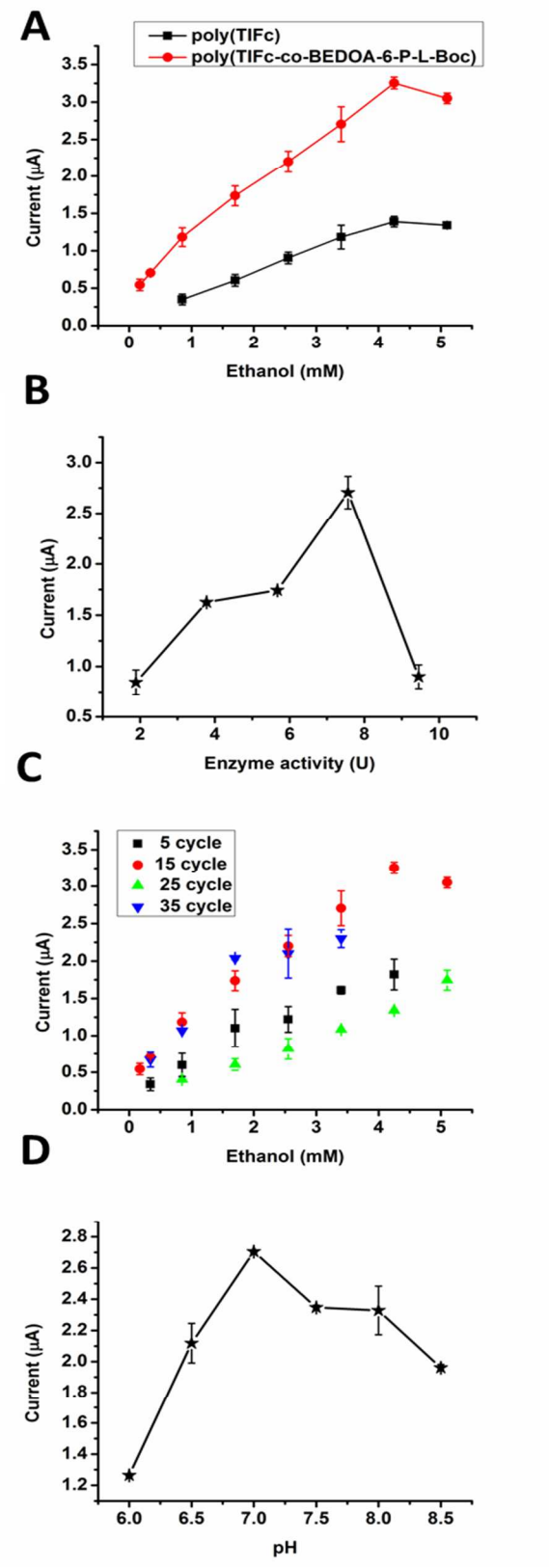

Figure 4. Effect of (A) polymer films as supporting matrix, (B) enzyme activity, (C) scan number, (D) pH on the biosensor response. Error bars show standard deviation (SD) of three measurements.

electrode exhibited a very small interfacial resistance. After coating the electrode surface with poly(TIFc-co-BEDOA-6-poly(L-Boc)), the semicircle diameter increased slightly due to the increase in thickness of the interface. The small resistance indicated a resistance of electron flow due to the addition of a layer on the electrode surface. Furthermore, polypeptide segments cause a decrease in conductivity effectively since the units interrupt the electron flow within the conjugation pathway. Hence, this increase in semicircle diameter is justified. After AOx was immobilized onto the coated electrode surface, the semicircle diameter increased significantly since the layer blocks the redox probe to diffuse toward the electrode. Moreover, since most biological molecules were poor electrical conductors at low frequencies, this increase in charge transfer resistance was the direct evidence of successful immobilization of enzyme on the modified transducer surface.

Scanning Electron Microscopy

The surface morphology of different electrode surfaces was monitored via SEM. Figure 5 A-C show SEM images of the conducting polymer coated graphite electrode (poly(TIFc)), polymeric structure bearing polypeptide segments coated graphite electrode poly(TIFc-co-BEDOA-6-poly(L-Boc)) and enzyme immobilized copolymer coated graphite electrode (poly(TIFc-co-BEDOA-6-poly(L-Boc))/AOx), respectively. In case of poly(TIFc) coated electrode, granular morphology was observed. On the other hand, poly(TIFc-co-BEDOA-6-poly(L-Boc)) exhibited completely different morphology. The copolymer film has an ability to cover the entire electrode surface homogeneously. By this way enhanced matrix properties is proved and it serves a platform which enzyme molecules are freely oriented. After biomolecule deposition, enzyme exhibits its bulky characteristics. This homogeneous 3D structure leads stabilization of the enzyme molecules, improving the biosensor performance. It can be clearly seen that the morphology of different prepared electrode alters significantly, referring copolymer formation and successful enzyme deposition.

Analytical Characterization

The analytical characterization of the biosensor was examined preparing an enzyme electrode under optimum conditions. Calibration curve for ethanol was plotted with respect to substrate concentration as given in Figure 6A. A perfect linearity was obtained between 0.17 mM and 4.25 mM ethanol as given with an equation; y=0.6485x+0.5329 and R^2= 0.9945 Limit of detection (LOD) was also calculated as 0.28 mM according to S/N = 3. Also, a typical amperometric response of the biosensor was given as an inset in Figure 6A.

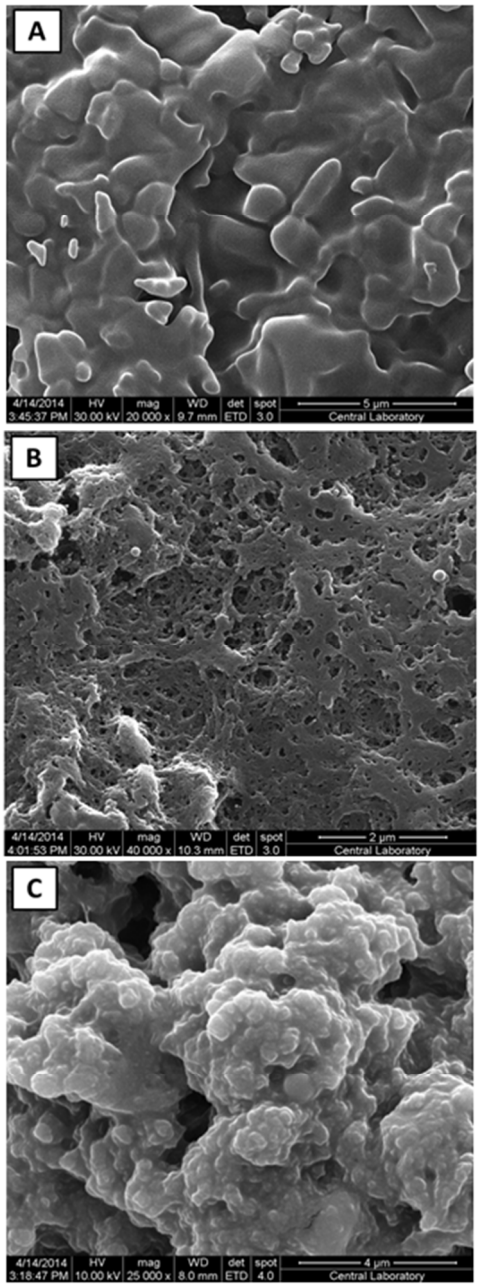

Figure 5. SEM images of (A) poly(TIFc); (B) poly(TIFc-co-BEDOA-6-poly(L-Boc)); (C) poly(TIFc-co-BEDOA-6-poly(L-Boc))/AOx under optimized conditions.

Moreover, the biosensor signals corresponding to 1.7 mM ethanol solution were measured for ten times in order to prove repeatability of the biosensor response. The standard deviation (SD) and the relative standard deviation (RSD) were calculated as 0.09 and 5.94 %, respectively. Also, operational stability of the biosensor was investigated under optimum conditions. During 5 h, 10 times current change was detected upon addition of 1.7 mM substrate and 16 % activity loss was found in the biosensor response.

Furthermore, kinetic parameters were characterized using Lineweaver-Burk plot.[50] The apparent Michaelis-Menten constant (K_M^{app}) and maxiumum current (I_{max}) were calculated as 2.67 mM and 2.98 μA, respectively. It is known that a low K_M^{app} value corresponds to high enzyme affinity toward the substrate. In this biosensing system, such a low K_M^{app} value was observed. A comparison among the present biosensor and several others reported in literature is given in Table 1. Thus, it is concluded that the immobilized alcohol oxidase exhibit higher affinity toward ethanol thanks to effective immobilization matrix. Successful design of the copolymer with different specialties of each unit improves the biosensor performance by serving adequate microenvironment for the enzyme. By this way, the interaction between the substrate and active site of enzyme was increased.

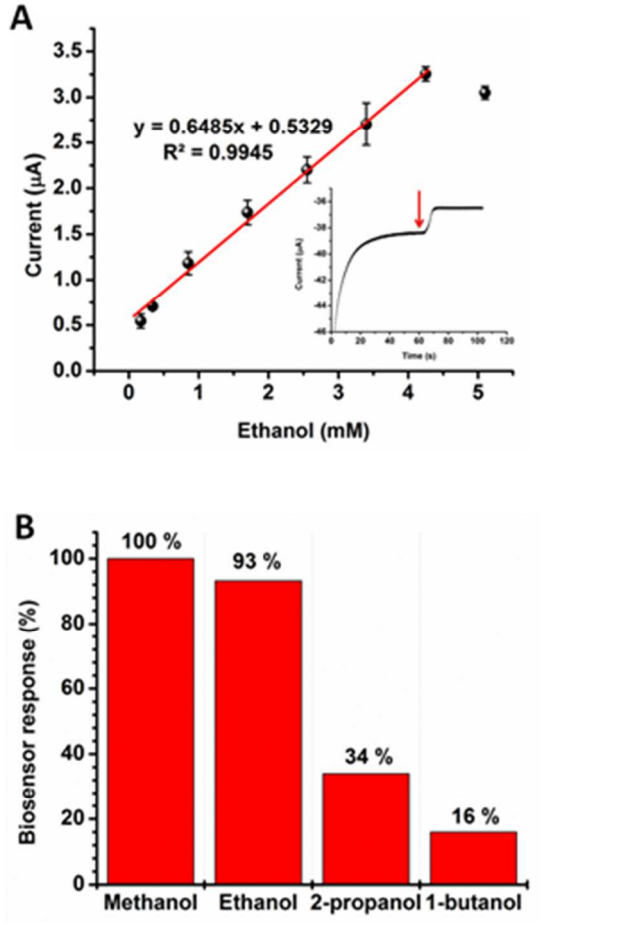

Figure 6. (A) Calibration curve for ethanol (in 50 mM phosphate buffer, pH 7.0, 25◦C,−0.7 V). Error bars show standard deviation of three measurements (A typical amperometric response to 1.7 mM ethanol in phosphate buffer, 50 mM, pH 7.0 given as inset); (B) Substrate selectivity of the biosensor (amperometric response of methanol accepted as 100%).

It was known that AOx contains different relative activities to several aliphatic alcohols.[57] To inquire substrate selectivity of the proposed biosensor, 1.7 mM of various alcohol substrates were tested and results were given in Figure 6B. The response of the biosensor to methanol was higher than the one for ethanol. Since methanol has the shortest alkyl chain and the final product in the enzymatic reaction is formaldehyde acting also as a substrate for AOx[58], the biosensor signal was amplified and the highest signal was recorded upon addition of methanol as the substrate. However, the fact that the biosensor gives higher response to methanol than to ethanol may not induce any problem for the detection of alcohol content in real food samples because the only content of alcohol in food products is expected to be ethanol. Thus, the enzyme electrode is potentially useful for the determination of ethanol in real food products. Moreover, as the alkyl chain of the alcohol increases, the biosensor response decreases since the substrates with longer chain cause steric hindrance while the substrate is reaching active site of the enzyme molecules. Thus, relative biosensor response decreases as the chain length increases.

Table 1. Comparison of some parameters of various alcohol biosensors reported in literature.

Matrices on electrodes	K_M^{app} (mM)	Linear range (mM)	Ref.
Au/PPYox/AOD-gel	5.30	Up to 0.75	[51]
Polypyrrole (PPy)/AOx	6.8	NR	[52]
f-MWCNT/poly(BIPN)/AOx	16.946	0.855 - 11.97	[53]
PNR/AOx	2.4	0-0.8	[54]
RPTP/PVI10-Os/PEG-DGE/AOx/CP5	9.5	NR	[55]
PMCCH/AOx	8.74	0.4–13.63	[56]
poly(TIFc-co-BEDOA-6-poly(L-Boc))/AOx	2.67	0.17–4.25	This work

Furthermore, the effect of potential interferents such as glucose, urea, cholesterol and ascorbic acid was investigated. For this purpose, these molecules (between 1 mM and 10 mM) were injected to the reaction cell under optimum conditions instead of ethanol as the substrate and no responses were recorded for these intereferents. Hence, the proposed sensing system can be used for real sample analysis even in the presence of such interferents in the sensing matrix.

Sample Application

The proposed sensing system was tested to analyze the alcohol content in several alcoholic beverages. The samples were

injected to the cell instead of ethanol substrate without any pretreatment. The responses of biosensor for each sample were recorded and values were estimated from the calibration curve. The experiments were performed at optimum conditions. As summarized in Table 2, the results are in really good agreement which approves the reliability and accuracy of the biosensor. Therefore, it is a reliable strategy for alcohol determination in real samples. Since the methods which are used for routine analysis have several drawbacks, the proposed biosensor design is a favorable method for real time analysis to investigate alcohol content in real alcoholic beverages. Hence it serves several advantages over traditional methods like simple measurement procedure, short response time, easy to fabricate and sufficient sensitivity and selectivity. Hence, the constructed biosensor is an accurate way for alcohol test in real samples.

Table 2. Ethanol detection in alcoholic beverages.

Sample	Ethanol Content		Relative error (%)
	Product label (%)	Poly(TIFc-co-BEDOA-6-poly(L-Boc))/AOx biosensor (%)	
B® Liquor	24.0	23.7	1.277
J® Whisky	40.0	36.7	8.99
Y® Wine	14.0	14.3	2.10
Y® Raki	45.0	46.1	2.39
S® Liquor	20.0	19.4	3.09
R® Wine	12.0	12.4	3.23

Experimental

Materials

Alcohol oxidase (AOx, E.C.1.1.3.13, 35 units/mg) from Pichiapastoris, methanol, NaClO4, LiClO4 Nε-Boc-L-lysine, tetrabutylammonium hydroxide, and diphenyl carbonate were purchased from Sigma-Aldrich and used with no further purification. Dichloromethane (DCM), acetonitrile (ACN) were purchased from Merck (Darmstadt, Germany). 2-Propanol and tert-butanol were obtained from (Merck). Ethanol (Carlo Erba) was used for the preparation of substrate solution (1.7 M) at room temperature. All chemicals for the synthesis of monomer were purchased from Aldrich except tetrahydrofuran (THF) which was obtained from Acros (Geel, Belgium, www.acros.com). THF was freshly dried over sodium and benzophenone just before the reactions. N,N-Dimethylacetamide (DMAc) and N,N-dimethylformamide (DMF) were purified by heating at 600C for 1 h over CaH2 followed by fractional distillation before use. All other chemicals were analytical grade. Reactions were performed under nitrogen atmosphere unless otherwise mentioned.

Measurements

All amperometric measurements were performed with the potentiostat EmStat (PalmSens, Houten, The Netherlands, www.palmsens.com) in a three-electrode cell configuration consisting of a graphite electrode (Ringsdorff Werke GmbH, Bonn, Germany, type RW001, 3.05 mm diameter and 13% porosity) as the working electrode. A platinum wire as the counter electrode and a silver wire as the pseudo reference electrode were used. Amperometric measurements were performed in a three-electrode system. In amperometric analyses, the data were given as the average of three measurements and standard derivations were recorded as ±SD. All measurements were performed at ambient conditions (25°C). For investigation of surface characteristic, scanning electron microscopy (SEM) (JEOL JSM-6400 model, Japan) was used. ATR-FTIR spectra were recorded on a Nicolet iS10 ATR-FTIR Spectrometer (Thermo Fisher Scientific Inc.). Electrochemical Impedance Spectroscpoy (EIS) was performed with a GAMRY Reference 600 (GAMRY Instruments Inc., Pennsylvania, USA). Structures were proven by nuclear magnetic resonance (NMR) spectra recorded on a Bruker Spectrospin Avance DPX-400 Spectrometer with trimethylsilane (TMS) as the internal reference. Gel-permeation chromatography (GPC) measurements were carried out in Viscotek GPCmax auto sampler system. Instrument was equipped with a pump (GPCmax, Viscotek Corp., Houston, TX), light-scattering detector (λ_0 = 670 nm, Model 270 dual detector, Viscotek Corp.) consisting of two scattering angles: 7° and 90° and the refractive (RI) index detector (VE 3580, Viscotek Corp.). Both detectors were calibrated with Polystyrene standards with a narrow molecular weight distribution. Three ViscoGEL GPC columns (G2000HHR, G3000HHR and G4000HHR) were employed with THF with a 1.0 mL min^{-1} flow rate at 30ºC. All data were analyzed using Viscotek OmniSEC Omni-01 software.

Synthesis of 6-(4,7-bis(2,3-dihydrothieno[3,4-b][1,4]dioxin-5-yl)-2H-benzo[d][1,2,3]triazol-2-yl)hexan-1-amine) (BEDOA-6)

The monomer, BEDOA-6 was synthesized according to a previously described method.[59] Firstly, 1H-benzo[d][1,2,3]triazole was substituted with alkyl chain to produce 2-(6-bromohexyl)-2H-benzo[d][1,2,3]triazole. After the product was dibrominated, the resultant 4,7-dibromo-2-(6-bromohexyl)-2H-benzo[d][1,2,3]triazole was coupled with 2,3-dihydrothieno[3,4-b][1,4]dioxine to acheieve 2-(6-bromohexyl)-4,7- bis(2,3-dihydrothieno[3,4-b][1,4]dioxin-5-yl)-2H-benzo[d][1,2,3]triazole. Then, the substituted product was reacted with potassium phthalimide to afford 2-(6-(4,7-bis(2,3-dihydrothieno[3,4-b][1,4]dioxin-5- yl)-2H-

benzo[d][1,2,3]triazol-2-yl)hexyl)isoindoline-1,3-dione. After addition of hydrazine monohydrate to the reaction, the desired monomer (BEDOA-6) was synthesized successfully.

Synthesis of N6-(tert-butoxycarbonyl)-N2-(phenoxycarbonyl)-L-lysine (Urethane derivative of N-Boc-L-lysine)

Synthetic route for urethane derivative of N-Boc-L-lysine is based on successive protection of the acid group of N-Boc-L-lysine with diphenyl carbonate by an ionic exchange reaction with the corresponding ammonium salt and N-carbamylation reaction. Thus, to a stirred suspension of N-boc-L-lysine (3.7g, 15.0 mmol) in methanol 15 mL, tetrabutylammonium hydroxide (37% in methanol) (10.5 g, 15.0 mmol) was slowly added at room temperature. After stirring for 1 h, the reaction mixture was concentrated under reduced pressure. The resulting residue was dissolved into acetonitrile (15 mL), and then the resulting solution was added drop wise to a stirred solution of diphenyl carbonate (3.21 g, 15.0 mmol) in acetonitrile (15 mL) at room temperature. After stirring the solution for 1h, distilled water (100 mL) was added into the resulting mixture and acidified to pH 2-3 with 1M HCl, and then extracted with ethyl acetate (3 × 20 mL). The combined organic layer was dried over Na2SO4, filtrated, and concentrated under reduced pressure. The crude product was purified with by column chromatography (eluting with a gradient from 30-70% ethyl acetate in n-hexane) and then concentrated to give target compound. Yield: 4.3 g (78%) as white powder. ^{1}H NMR (400 MHz, DMSO-d_6, δ, ppm): 1.26-1.47 (s, 13H), 1.58-1.82 (m, 2H), 2.84-2.99 (m, 2H), 3.90-3.98 (m, 1H), 6.74-6.83 (m, 1H), 7.08 (d, 2H, J = 7.7 Hz), 7.19 (t, 1H, J = 7.4 Hz), 7.37 (t, 2H, 7.9 Hz), 8.04 (d, 1H, J = 7.9 Hz). ^{13}C NMR (100 MHz, DMSO-d_6, δ, ppm): 22.95, 28.30, 29.09, 30.40, 54.02, 77.37, 121.60, 124.97, 129.27, 150.97, 154.43, 155.59, 173.61. (-NH-CH_2-: overlapped by the DMSO-d_6 signal).

Synthesis of electroactive BEDOA-6-poly(L-Boc)

Polymerization of the urethane derivative of N-Boc-L-lysine proceeded in the presence of BEDOA-6 as initiator in DMAc in a one-pot reaction through in situ intramolecular cyclization followed by a ring-opening reaction with CO2 elimination. Typical procedure: urethane derivative of N-Boc-L-lysine (916 mg, 2.5 mmol) was dissolved in anhydrous DMAc (2.5 mL), and the solution was added into a schlenk tube. After the addition of the BEDOA-6 (250 Mg 0.5 mmol) resulting mixture was stirred at 60 oC for 24 h under argon atmosphere. The reaction mixture was cooled to room temperature, and poured into diethyl ether (100 mL). Slightly sticky white participate was dissolved in a small amount of THF and then dried under vacuum to yield 85% as white powder. GPC: Mn = 17000, M_w/M_n = 1.62. ^{1}H NMR (500 MHz, $CDCl_3$, δ, ppm): 1.79 – 1.33 (br, 21H), 2.07 – 1.80 (br, 2H), 3.09 (s, 4H), 4.03 – 3.70 (br, 1H), 4.30 (s, 2H), 4.38 (s, 2H), 4.80 (s, 2H), 5.16 (br, 2H), 6.52 (s, 2H), 8.11 (s, 4H), 8.52 – 7.87 (br, 2H).

Synthesis of 2-ferrocenyl-4,7-di(thiophen-2-yl)-1H-benzo[d]imidazole (TIFc)

4,7-Dibromobenzothiadiazole,[60] 6-dibromobenzene-1,2-diamine,[61] tributyl(thiophen-2-yl)stannane[62] were synthesized according to the literature procedures. Bromination of benzothiadizaole was followed by the reduction to yield 3,6-dibromobenzene-1,2-diamine. The product was reacted with ferrocene aldehyde by the help of iodine catalyst as described in literature[63] and then coupled with tributyl(thiophen-2-yl)stannane via Stille coupling reaction and desired monomer 2-ferrocenyl-4,7-di(thiophen-2-yl)-1H-benzo[d]imidazole (TIFc) was obtained (Scheme S3).

4,7-Dibromo-2-ferrocenyl-1H-benzo[d]imidazole (500 mg, 1.08 mmol) and tributyl(thiophen-2-yl)stannane (886 mg 2.38 mmol) were dissolved in dry THF and stirred under argon flow for 20 minutes. Then dichlorobis(triphenyl phosphine)palladium(II) (70 mg, 0.064 mmol) was added and the reaction was refluxed overnight. After removing the solvent under reduced pressure, the residue was subjected to column chromatography on silica gel and a yellowish-brown solid was obtained (310 mg yield:61%). ^{1}H-NMR (400 MHz, $CDCl_3$, δ): 4.14(s, 5H), 4.50(dd, 2H), 5.32(dd, 2H), 7.20-7.35(m,3H), 7.52-7.73(m, 4H) 8.23(s, 1H), 12.19 (s, 1H). ^{13}C (300Mz, DMSO, δ): 66.19, 69.50, 69.83, 73.97, 117.10, 118.80, 121.90, 122.79, 125.75, 126.12, 127.63, 128.40, 132.35, 139.63, 140.34, 141.02, 154.58.

Electro copolymerization of BEDOA-6-poly(L-Boc) and TIFc

Prior to polymerization, spectroscopic grade graphite rods were polished on an emery paper and washed thoroughly with distilled water. After the cleaning procedure, electrochemical copolymerization and film deposition was carried out on the graphite electrode via cyclic voltammetry. A mixture of TIFc and BEDOA-6-poly(L-Boc) solution was subjected to cyclic voltammetry (CV) for 15 cycles in 0.1 M $NaClO_4$/$LiClO_4$/ACN electrolyte/solvent system by scanning the potential between -0.2 V and 0.8 V. Polymer coated electrode was rinsed with distilled water to remove possible impurities. Similar experimental procedure was applied for the polymerization of TIFc in the absence of BEDOA-6-poly(L-Boc).

Immobilization of enzyme, crosslinking and biosensing

To immobilize the enzyme, 3 µL of AOx solution (50 mM pH 7.0 sodium buffer solution containing AOX) was spread over the polymer coated electrode surface. Then, glutaraldehyde solution (5 µL, 1%, in 50 mM phosphate buffer, pH 7.0) was casted on the electrode as the cross linker agent and the

Journal Name RSCPublishing

ARTICLE

electrode was allowed to dry for 2 h at room temperature. Before use, the electrode was rinsed with pH 7.0 phosphate buffer solution to remove loosely bound enzymes from the electrode. It was stored at 4°C when not in use.

Amperometric biosensor measurements were performed at ambient conditions in a cell containing 5 ml buffer solution under a mild stirring. After the electrodes were initially placed in the cell, the signal baseline reached a steady state and certain amount of substrate was injected to the reaction cell. At this point the response of the biosensor was measured by detecting the current change when equilibrium was established. The electrode was washed with distilled water and buffer was refreshed after each measurement.

Conclusion

In this study, we successfully achieved a complex macromolecular architecture based on a conjugated copolymer to construct a novel biosensor. Conducting copolymers possessing both polypeptide and ferrocene units were prepared by electro copolymerization and used as an immobilization platform of AOx. While polypeptide segments created an excellent biocompatible environment for biomolecule deposition as well as enabling covalent attachment of the enzyme, the ferrocene units provided enhanced biosensor performance without any leaching. The constructed biosensor reflecting the advantage of each component was characterized in detail by FTIR, SEM, and EIS analyses. The biosensor was used to analyze ethanol content in real sample and proposed as an alternative sensing system for ethanol analysis in alcoholic beverages. We anticipate the described approach will be applicable to numerous other types of enzymes with different sensing abilities. The combination of polypeptides with conjugated polymers by means of electro copolymerization has potential use in the construction of new biological macromolecular architectures.

Notes and references

[a] *Department of Chemistry, Middle East Technical University, 06800 Ankara, Turkey*
[b] *Department of Chemistry, Faculty of Science and Letters, Istanbul Technical University, 34469 Istanbul, Turkey.*
[c] *Institute of Science and Technology, Department of Advanced Technologies, Gazi University, 06570 Ankara, Turkey.*
[d] *Molecular Engineering Institute, Kinki University, 11-6 Kayanomori, Iizuka, Fukuoka 820-8555, Japan.*
[e] *Department of Polymer Science and Technology, Middle East Technical University, 06800 Ankara, Turkey*
[f] *The Center for Solar Energy Research and Applications (GUNAM), Middle East Technical University, 06800 Ankara, Turkey*
[g] *Department of Biotechnology, Middle East Technical University, 06800 Ankara, Turkey*

† Electronic Supplementary Information (ESI) available: Synthetic pathway of BEDOA-6, N-Boc-L-lysine, TIFc. ATR-FTIR spectra of poly(TIFc), poly(TIFc-co- BEDOA-6-poly (L-Boc)) and Typical Nyquist plots.See DOI: 10.1039/b000000x/

1 Y. Li, Z. Pan, L. Miao, Y. Xing, C. Li and Y. Chen, *Polym. Chem.,* 2014, **5**, 330; H. Hoppe and N. S. Sariciftci, *J. Mater. Res*., 2004, **19**, 1924; K. Y. Seah, J. Li, K-H. Ong, H-S. Tan, S-L. Lim, H-K. Wong and Z.-K. Chen*, *Polym. Chem.,* 2013, **4**, 260.
2 A. Ramanaviciene, W. Schuhmann and A. Ramanavicius, *Colloid. Surf. B*, 2006, **48**, 159; R. Graciaa and D. Mecerreyes, *Polym. Chem.,* 2013, **4**, 2206.
3 W. Schuhmann, *Microchim. Acta*, 1995, **21**, 1.
4 K.V. Santhanam, *Pure Appl. Chem*., 1998, **70**, 1259; J. C. Claussen , A. Kumar , D. B. Jaroch , M. H. Khawaja , A. B. Hibbard , D. M. Porterfield and T. S. Fisher, *Adv. Funct. Mater.,* 2012, **22**, 3399.
5 Y. Xian, Y. Hu, F. Liu, Y. Xian, H. Wang and L. Jin, *Biosens. Bioelectron*, 2006, **21**, 1996.
6 B.D. MAlhotra, A. Chaubey and S.P.Singh, *Anal. Chim. Acta*, 2006, **578**, 59; B. Wang, C. Zhu, L. Liu, F. Lv, Q. Yang and S. Wang, *Polym. Chem.,* 2013, **4**, 5212.
7 Jun Ling, Hui Peng and Zhiquan Shen, *J. Polym. Sci., Part A: Polym. Chem.,* 2012, **50**, 3743.
8 R. Obeid, C. Scholz, *Biomacromolecules*, 2011, **12**, 3797.
9 Y. Dai, M. Xu, J. Wei, H. Zhang and Y. Chen, *Appl. Surf. Sci*., 2012, **258**, 2850.
10 T. Tsuruta, *Adv. Polym. Sci.,* 1996, **126**, 1 ; J. Jagur-Grodzinski, *React. Funct. Polym*., 1999, **39**, 99.
11 O. Pillai and R. Panchagnula, *Curr. Opin. Chem. Biol*., 2001, **5**, 447.
12 K. Ishikawa and T. Endo, *J. Am. Chem. Soc*., 1988, **110**, 2016.
13 M.T. Krejchi, E.D. Atkins, A.J. Waddon, M.J. Fournier, T.L. Mason and D.A. Tirrell, *Science*, 1994, **265**, 1427.
14 T. Koga, M. Matsuoka and N. Higashi, *J Am Chem Soc*, 2005, **127**, 17596.
15 F.E. Appoh, D.S. Thomas and H.B. Kraatz, *Macromolecul*es, 2006, **39**, 5629.
16 S. Ohsawa, B. Barkakaty, A. Sudo and T. Endo, *J. Polym. Sci., Part A: Polym. Chem.,* 2012, **50**, 1281.
17 K.-S. Krannig and H. Schlaad, *J. Am. Chem. Soc*., 2012, **134**, 18542.
18 T.J. Deming, *J. Am. Chem. Soc*., 1997, **119**, 2759.
19 S. Yamada, K. Koga and T. Endo, *J. Polym. Sci., Part A: Polym. Chem,* 2012, **50**, 2527.
20 K. Koga, A. Sudo, H. Nishida and T. Endo, *J. Polym. Sci., Part A: Polym. Chem,* 2009, **47**, 3839.

21 S. Yamada, K. Koga, T. Endo and *J. Polym. Sci., Part A: Polym. Chem.,* 2012, **50**, 2527.
22 T.J. Deming, Polypeptide and polypeptide hybrid copolymer synthesis via NCA polymerization. In *Peptide Hybrid Polymers*, H.A. Klok, H. Schlaad, Eds. 2006; Vol. 202, pp 1-18.
23 T.J. Deming, *Advanced Materials,* 1997, **9**, 299.
24 Y. Kamei, A. Nagai, A. Sudo, H. Nishida, K. Kikukawa, T. Endo, *J. Polym. Sci., Part A: Polym. Chem,* **2008**, 46, 2649.
25 Y. Kamei, A. Sudo, H. Nishida, K. Kikukawa and T. Endo, *Polym. Bull.,* 2008, **60**, 625.
26 K. Koga, A. Sudo and T. Endo, *J. Polym. Sci., Part A: Polym. Chem,* 2010, **48**, 4351.
27 Y. Kamei, A. Sudo, H. Nishida, K. Kikukawa and T. Endo, *J. Polym. Sci., Part A: Polym. Chem.,* 2008, **46**, 2525.
28 J. Sun and H. Schlaad, *Macromolecules,* 2010, **43**, 4445.
29 J.W. Robinson and H. Schlaad, *Chem. Commun.,* 2012, **48**, 7835.
30 T. Aliferis, H. Iatrou and N. Hadjichristidis, *Biomacromolecules,* 2004, **5**, 1653.
31 H. Iatrou, H. Frielinghaus, S. Hanski, N. Ferderigos, J. Ruokolainen, O Ikkala, D. Richter, J. Mays and N. Hadjichristidis, *Biomacromolecules,* 2007, **8**, 2173.
32 N. Hadjichristidis, H. Iatrou, M. Pitsikalis and G. Sakellariou, *Chem. Rev.,* 2009, **109**, 5528.
33 J. Qiu, W. Zhou, J. Guo, R. Wang and R. Liang, *Anal. Biochem*., 2009, **385**, 264.
34 J. Chen, A.K. Burrell, G.E. Collis, D.L. Officer, G.F. Swiegers, C.O. Too and G.G. Wallace, *Electrochim. Acta*, 2002, **47**, 2715.
35 M.Senel, E. Cevik and M. F. Abasıyanık, *Sens. Actuat. B-Chem*., 2010, **145**, 444.
36 N. C. Foulds and R. C. Lowe, *Anal. Chem*., 1988, **60**, 2473.
37 A. M. Azevedo, D. Miguel, F. Prazeres, M.S. Joaquim, M.S. Cabral and L. P. Fonseca, *Biosens. Bioelectron.,* 2005, **21**, 235.
38 S. Alkan, L. Toppare, Y. Hepuzer and Y. Yagci, *J. Polym. Sci., Part A: Polym. Chem*, 1999**, 37**, 4218.
39 E. Unur, L. Toppare, Y. Yagci and F. Yilmaz, *Mater. Chem. Phys*., 2005, **91**, 261.
40 H.B. Yildiz, S. Kiralp, L. Toppare and Y. Yagci, K. *Mater. Chem. Phys*., 2006, **100**, 124.
41 I. Kerman, L. Toppare, F. Yilmaz and Y. Yagci, *J. Macromol. Sci., Pure Appl. Chem*., 2005, **A42**, 509.
42 M. Ak, B. Gacal, B. Kiskan, Y. Yagci and L. Toppare, *Polymer*, 2008, **49**, 2202.
43 H. Akbulut, M. Yavuz, E. Guler, D.O. Demirkol, T. Endo, S. Yamada, S. Timur and Y. Yagci, *Polym. Chem*, 2014, **5**, 3929.
44 L. Guan, Z. Shi, M. Li and Z. Gu, *Carbon*, 2005, **43**, 2780.
45 M. Rutnakornpituk, N. Puangsin, P. Theamdee, B. Rutnakornpituk and U. Wichai, *Polymer*, 2011, **52**, 987.
46 E. Yildiz, P. Camurlu, C. Tanyeli, I. Akhmedov and L. Toppare, *J. Electroanal. Chem*., 2008, **612**, 247.
47 S. Tuncagil, D. Odaci, E. Yildiz, S. Timur and L. Toppare, *Sens. Actuat. B-Chem*., **2009**, 137, 42.
48 F. Lisdat and D. Schäfer, *Anal. Bioanal. Chem*., 2008, **391**, 1555.
49 E.P. Randviir and C.E. Banks, *Anal. Methods*, 2013, **5**, 1098.
50 L. Lineweaver and D. Burk, *J. Amer. Chem. Soc.,* 1934, **56**, 658.
51 D. Carelli, D. Centonze, A. De Giglio, M. Quinto and P.G. Zambonin, *Anal. Chim. Acta*, 2006, **565**, 27.
52 H. B. Yildiz and L. Toppare, *Biosens. Bioelectron*., 2006, **21**, 2306.
53 S. Soylemez, F. Ekiz Kanik, S. Demirci Uzun, S. O. Hacioglu and L. Toppare, *J. Mater. Chem. B*, 2014, **2**, 511.
54 M.M. Barsan and C. M.A. Brett, *Talanta,* 2008, **74**, 1505.
55 I. S. Alpeeva, A. Vilkanauskyte, B. Ngounou, E.Csoregi, I. Yu. Sakharov, M. Gonchar and W. Schuhmann, *Microchim Acta*, 2005, **152**, 21.
56 N. C. Kekec, F. Ekiz Kanik, Y. Arslan Udum, C. Gundogdu Hizliates, Y. Ergun and L. Toppare, *Sens. Actuat. B-Chem*, 2014, **193**, 306.
57 F.W. Janssen and H,W. Ruelius, *Biochim. Biophys. Acta,* 1968, **151**, 330.
58 A.R. Vijayakumar, E. Csöregi, A. Heller and L. Gorton, *Anal. Chim. Acta,* 1996, **327**, 223.
59 M. Kesik, O. Kocer, F. Ekiz Kanik, N. Akbasoglu Unlu, E. Rende, E. Aslan-Gurel, R. M. Rossi, Y. Arslan Udum and L. Toppare, *Electroanalysi,s* 2013, **25**, 1995.
60 B. A. DaSilveira Neto, A. Santana Lopes, G. Ebeling, R. S. Gonçalves, V. E.U. Costa, F.H. Quina and J. Dupont, *Tetrahedron*, 2005, **61**, 10975.
61 Y. Tsubata, T. Suzuki, T. Miyashi and Y.Yamashita, *J. Org. Chem*., 1992, **57**, 6749.
62 X. Guo and D. M. Watson, *Org. Letters*, 2008, **10**, 5333.
63 H. Akpınar, A. Balan, D. Baran, E.K. Ünver and L. Toppare, *Polymer*, 2010, **51**, 6123.